

Continuous laser printing of surface relief microstructures on photomechanically-responsive azopolymer films using structured optical polarization

O. Senel^a, B. Gruppuso^b, J. Strobelt^b, and D. J. McGee*^b

^aDepartment of Physics, Berliner Hochschule für Technik, 13353 Berlin, Germany; ^bDepartment of Physics, The College of New Jersey, Ewing, NJ, USA 08628

ABSTRACT

Direct laser writing of surface relief microstructures on azopolymer films using structured polarization is an emerging technology for the fabrication of diffractive optics. Films are photopatterned with 488 nm laser light and a spatial light modulator (SLM) configured as a polarization modulator. The structures require no post-exposure processing, and can be replicated using nanoimprint lithography. A limitation of this method is that typical exposure areas are of order 1 mm². Larger areas require XY stepping of the film, degrading the diffractive functionality due to the stitched boundaries between exposures. Here we report that continuous scanning of the film in the structured polarized illumination reduces boundary structure effects. This has been previously demonstrated in photochemical materials such as photoresist, and it is effective in photomechanical azopolymers since the characteristically slow response enables a surface-averaging that results in relief gratings of highly uniform amplitude. Additionally, the surface relief amplitude and period can be continuously varied via direct programming of the SLM and scan rate. We use the system to fabricate a variety of sinusoidal surface relief gratings of area 25 mm² which were replicated via nanoimprint lithography and which exhibited first order diffraction efficiencies approaching 33% at 633 nm. We also fabricated chirped gratings designed to diffract RGB along a common direction in first order, with custom color generation based on grating area.

Keywords: diffractive optical element, surface relief grating, photopolymer, laser lithography

1. INTRODUCTION

Optical microstructures function as diffractive elements in photonic devices such as spectrometers, virtual reality displays, and anti-counterfeiting devices.^{1,2} Such microstructures, also called surface relief gratings (SRG), are typically fabricated using a laser source to generate a topographical surface distortion on a photoresponsive thin film, which is subsequently replicated using imprint lithography for volume production.

Laser-writing of SRGs generally utilizes either laser interferometry or optical diffraction. In laser interferometry, a laser beam is divided and recombined onto the surface of the photoresponsive film. This produces SRGs with uniform periodicity and low light scattering. The area of the SRG written is the area of the intersecting laser beams on the film surface, typically of order 1 mm², and often smaller. For larger area structures, the laser beams can be expanded (adding complexity to correct for distorted optical wavefronts), or the film can be mechanically scanned.^{3,4} A significant limitation of laser interferometry is the need for highly coherent laser sources and a mechanically stable environment. A separate constraint is that a given optomechanical writing arrangement produces an SRG of a single, fixed periodicity. To change the SRG requires a change in the intersection angle of the writing laser beams. Optically diffractive processes are an alternative for SRG fabrication in which the beam division is accomplished with a diffractive element, such as a diffraction grating or spatial light modulator (SLM).^{5,6} This somewhat relaxes the environmental stability requirements inherent in interferometric processes. Perhaps most advantageous is that SLM-based processes do not require optomechanical re-alignment to vary the SRG period or orientation. Common to both processes is the photoresponsive film, which is typically a photoresist.^{7,8} Exposed portions of the film undergo a photochemical change, which is converted to a surface relief pattern by wet chemical processing.

*mcgeed@tcnj.edu

Multiple factors limit widespread use of these materials. Because the films respond to light with a photochemical change, it is impossible to alter or otherwise correct the SRG once exposed. For similar reasons, ambient light must be eliminated from the fabrication setup. The chemical development adds additional complexity, with the depth and shape of the resulting SRG being sensitive to this processing step.

As an alternative, azobenzene-polymers with a photomechanical response have demonstrated potential for SRG fabrication. Spatially periodic linearly polarized light drives an orientational response of the azobenzene, exerting a periodic torque on the polymer. This ultimately distorts the film surface into a surface relief with the same period as the illumination. The inherent photomechanical response means that the surface relief appears directly in response to polarized light, its evolution can be viewed in real time and in ambient lighting, and it is available for replication immediately after exposure. While SRG fabrication with these azopolymers has been studied extensively⁹⁻¹⁵, nearly all of it has been done using laser-interferometry with the resulting grating area too limited for widespread use in applications. However, recent experiments using SLM-based systems¹⁶⁻¹⁹ and mechanical scanning^{20,21} have provided the proof-of-concept results that some combination of photomechanical azopolymers and diffractive writing processes using an SLM can evolve into a practical platform for facile and inexpensive production of large-area SRGs.

Here we demonstrate a laser-writing process for SRGs using a continuously moving azopolymer film in which the film speed controls the surface depth modulation and an SLM configured as a polarization modulator provides a surface pattern of programmable periodicity. Sinusoidal SRGs of area 25 mm^2 , $2.0 \mu\text{m}$ period, and amplitudes up to 670 nm were fabricated and replicated. Diffraction efficiencies of the transparent replica gratings were of order 30%, with the diffracted modes showing none of the higher-order structure commonly observed with gratings printed with a stepwise stitching pattern. We likewise exploited the programmable periodicity afforded by the SLM to continuously print SRGs that diffracted red, green, and blue modes along a common direction, demonstrating the potential of this process in structured color applications. An overall observation is that the slow photomechanical response provides a powerful averaging effect on optomechanical perturbations that might otherwise impact the SRG amplitude uniformity, which was observed here to be $\pm 4\%$ over the grating area. The 25 mm^2 SRG area is constrained only by the translational limits of the film scanning motors, demonstrating that this combination of photomechanically-responsive film and SLM-polarization projector is a viable platform for the scalable production of large-area optical surface microstructures.

2. EXPERIMENT

The experimental setup for continuous laser-printing of surface relief microstructures is shown in Figure 1. A diode-pumped solid-state laser at 488 nm illuminates a reflective SLM. The polarization-modulated light is projected onto the azopolymer film, forming a $130 \mu\text{m} \times 80 \mu\text{m}$ image at the film surface. The film is the azopolymer 4-hydroxy-40-dimethylaminoazobenzene and poly(4-vinylpyridine) and is more fully described in ref. 11. Films of order $1 \mu\text{m}$ thickness were spin coated on glass substrates and were used for all results reported here.

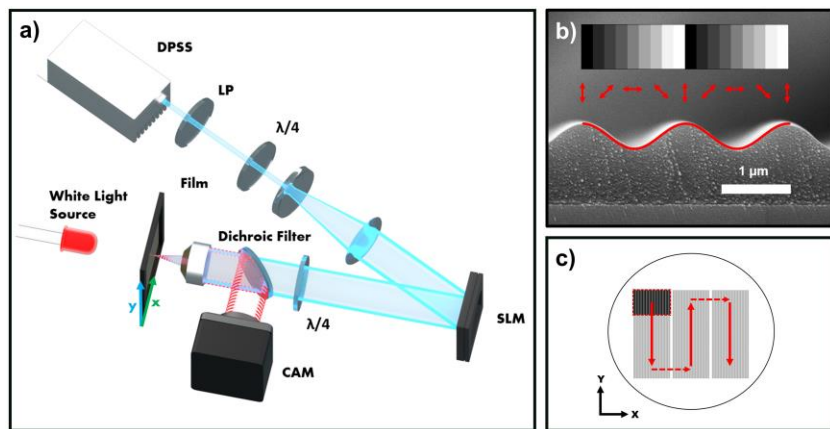
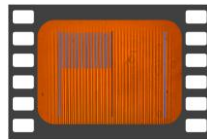


Figure 1. Experimental setup for continuous printing of SRG on azopolymer film. (a) 488 nm light from DPSS laser is polarization modulated by SLM and crossed $\lambda/4$ waveplates and imaged onto film surface. (b) Grayscale addressed to SLM generates spatially structured polarization (red), which drives sinusoidal surface relief. (c) Film is mounted in motorized XY stage and follows raster pattern shown.

The film is mounted in an XY motor stage with translational speeds ranging from 2 $\mu\text{m/s}$ to 20 $\mu\text{m/s}$. The printed surface structure can be viewed *in situ* using the white light source, dichroic mirror, and camera in a confocal imaging configuration. The SLM is a liquid crystal on silicon device with 1920×1152 pixels and is situated between crossed quarter-wave plates. This configuration rotates the polarization of an incident laser beam at each pixel according to the optical retardation of the SLM. Addressing the SLM with the gray scale pattern shown in Figure 1b subsequently illuminates the film surface with the corresponding spatially periodic polarization. This drives a photomechanical film response, resulting in a surface relief grating of the same period and with an approximately sinusoidal depth profile.

To print large-area structures, the film is continuously translated at constant speed parallel to the grating lines (i.e. perpendicular to the grating vector) while being illuminated with the spatial polarization distribution provided by the SLM. This effectively results in a rectangular scanning spot of $130 \mu\text{m} \times 80 \mu\text{m}$. For a typical linear SRG the scan follows the raster pattern shown in Figure 1(c). When the film reaches the end of a column of laser-printing, it is translated laterally by an integer multiple of the SRG period and the scanning process repeated. For the results presented here, the lateral stepping distance was $130 \mu\text{m}$ and the optical intensity remained constant at either $45 \times 10^3 \text{ mW/cm}^2$ or $90 \times 10^3 \text{ mW/cm}^2$ for the entire raster.

Video 1 was captured using the confocal *in situ* imaging setup and shows the film surface moving at a fixed speed of 8.5 $\mu\text{m/s}$ as it is exposed to the $130 \mu\text{m} \times 80 \mu\text{m}$ structured polarization pattern from the SLM. The continuous writing of the surface relief pattern is clearly visible, and the motion is identifiable through the appearance of random imperfections in the film surface. During the translation, the periodicity of the pattern on the SLM is varied, demonstrating the versatility of this system in writing continuously chirped gratings.



Video 1. Video showing continuous printing of SRG. <http://dx.doi.org/10.1117/12.3000374>

3. RESULTS

Atomic force microscopy (AFM) results of continuously printed SRGS are shown in Figure 2. The film was translated at constant speed during the exposure process, following the raster pattern shown in Figure 1.

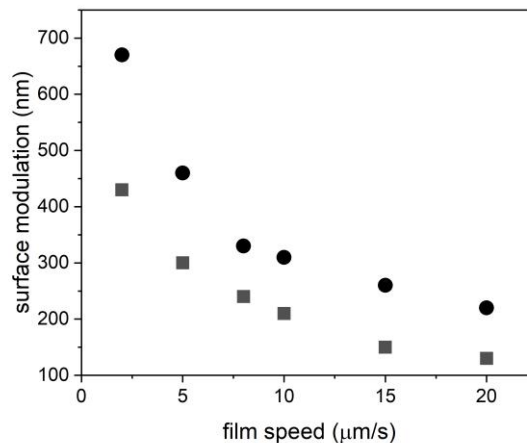


Figure 2. AFM measurements of SRG vs. film speed during exposure. Film was continuously translated parallel to grating lines for total distance of 1.0 mm. Exposure intensity was $45 \times 10^3 \text{ mW/cm}^2$ (squares) and $90 \times 10^3 \text{ mW/cm}^2$ (circles).

Here, the SLM was addressed with a grayscale pattern of 84 cycles, which when projected onto the film surface resulted in a linear polarization period of $2.0 \mu\text{m}$ over an exposure area of $130 \mu\text{m} \times 80 \mu\text{m}$. The total area of each SRG in this demonstration is $0.26 \text{ mm} \times 1.00 \text{ mm}$ and corresponds to 2 printed columns. This was repeated at speeds ranging from 2

$\mu\text{m/s}$ to $20 \mu\text{m/s}$. After each SRG printing process, the film was removed and characterized by AFM. While the summary results in Figure 2 demonstrate that translational speed during exposure can control surface grating amplitude, it is important to note that a wider range of amplitudes and periods are possible by changing the optical power, film speed, and period addressed to the SLM.

Guided by these results, we expanded the raster scan area to $5 \text{ mm} \times 5 \text{ mm}$. Figure 3 shows representative results for a 350 nm amplitude grating. The photograph shows the film surface illuminated under diffuse light; the film has no reflective overcoat. The amplitude and period were measured by AFM at 5 random locations across the film. The amplitude variation was less than $\pm 4\%$ while the period variation was essentially negligible.

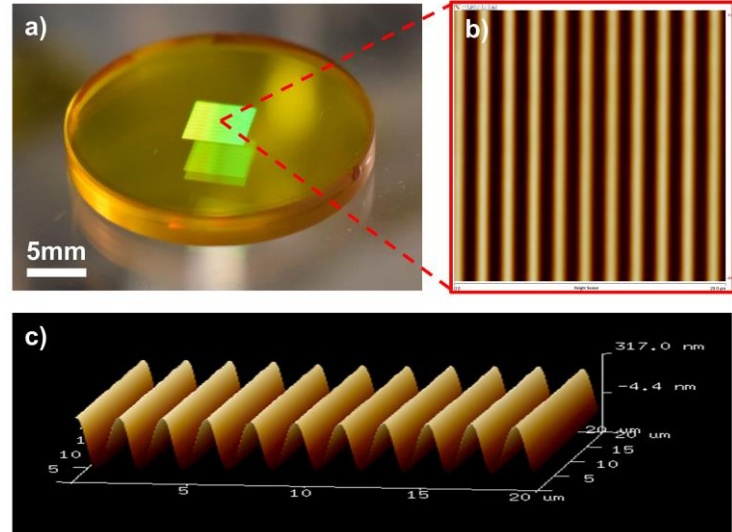


Figure 3. (a) $5 \text{ mm} \times 5 \text{ mm}$ SRG printed using setup of Figure 1 at film speed of $7 \mu\text{m/s}$. Azopolymer film is viewed in diffuse light; film stored in ambient conditions with no protective or reflective overcoat and photographed 6 months after fabrication. (b) and (c) are AFM scans over a $20 \mu\text{m} \times 20 \mu\text{m}$ area showing 350 nm surface modulation and $2.0 \mu\text{m}$ period.

To demonstrate the viability of this process to produce diffractive optical components in volume, the SRG of Fig. 3 was replicated with nanoimprint lithography and characterized with diffraction efficiency measurements. The replication process is shown in Fig. 4(a) and begins with the production of a flexible master mold from the original microstructure.

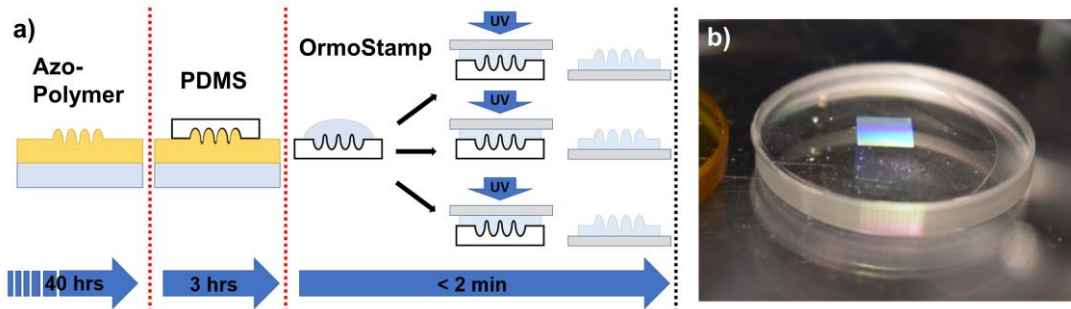


Figure 4. (a) Replication process flow for continuously printed SRG. (b) OrmoStamp replica of SRG in Fig. 3(a) viewed in diffuse light.

Polydimethylsiloxane (PDMS) was deposited onto the SRG, cured at 60 deg C for 2 hours, and removed to reveal a negative master. For the final positive replicated structure, a UV-curable inorganic-organic hybrid polymer system (OrmoStamp) was used. This was deposited on the PDMS master mold along with a glass substrate and UV cured for 2 minutes. Removal from the PDMS master mold revealed an optically clear and mechanically robust copy of the original microstructure as shown in Figure 4(b). Atomic force microscopy comparisons of the original microstructure and the OrmoStamp replica show excellent reproduction fidelity, with the only observable difference being a 10% loss in the SRG amplitude.

Additional 5 mm x 5 mm SRGs (each at a different write speed) were fabricated and replicated in OrmoStamp. Figure 5(a) shows the diffraction efficiency of these replicated gratings measured at 0.633 μm , 0.532 μm , and 0.488 μm , with the maximum efficiencies of order 30%. Figure 5(b) shows a 5 mm x 5 mm grating replicated in Ormostamp (400 nm surface modulation). The replicated grating (foreground) is illuminated with collinear lasers of wavelength 0.633 μm , 0.532 μm , and 0.488 μm (equal power) with the resulting +/- 1 diffracted orders shown on the glass screen in the background. Of particular note is the absence of visible higher order structure on the diffracted modes, as is commonly observed with gratings printed with a tiled stitching pattern.

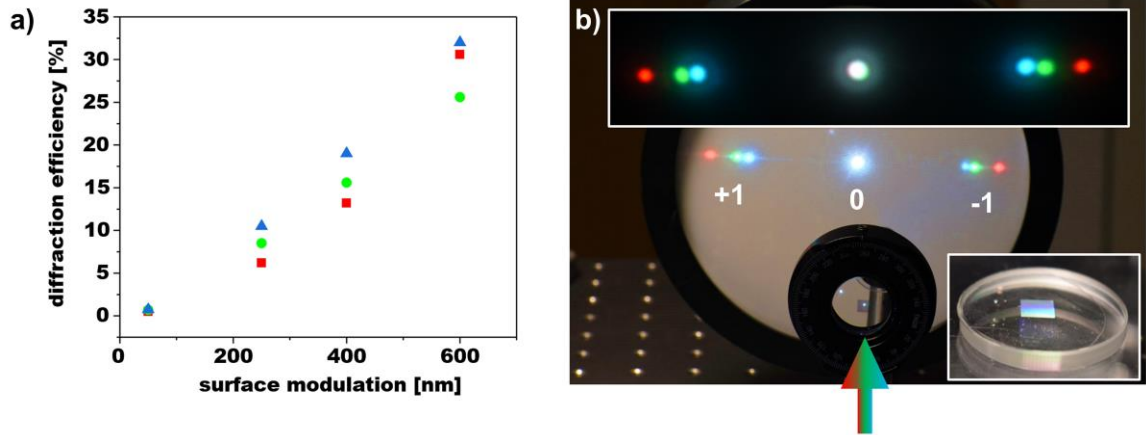


Figure 5. (a) Measured diffraction efficiency at 0.633 μm (red), 0.532 μm (green), and 0.488 μm (blue) for 4 OrmoStamp SRGs as a function of surface modulation. Each SRG had area 5 mm x 5 mm. (b) OrmoStamp replica SRG (400 nm surface modulation) of area 5 mm x 5 mm illuminated at normal incidence with collinear 0.633 μm , 0.532 μm , and 0.488 μm laser beams of equal 4 mW power. In foreground, grating is visible in center of rotational stage. Diffracted +/- 1 modes visible on glass screen in background. Top inset shows closeup view of diffracted modes, indicating no visible higher-order structuring.

One application that exploits the programmable periodicity of this fabrication process is structured color. Consider that the 130 μm x 80 μm scanning area produced by the SLM can be subdivided into 3 regions, each with a unique period d_r , d_g , and d_b and area A_r , A_g , and A_b . Defining the period relationship among the 3 regions as $\lambda_r/d_r = \lambda_g/d_g = \lambda_b/d_b$ (where $\lambda_r = 0.633 \mu\text{m}$, $\lambda_g = 0.532 \mu\text{m}$, and $\lambda_b = 0.488 \mu\text{m}$) produces a 1st order diffracted mode in which red, green and blue light propagate at a common angle as shown in Figure 6(a).

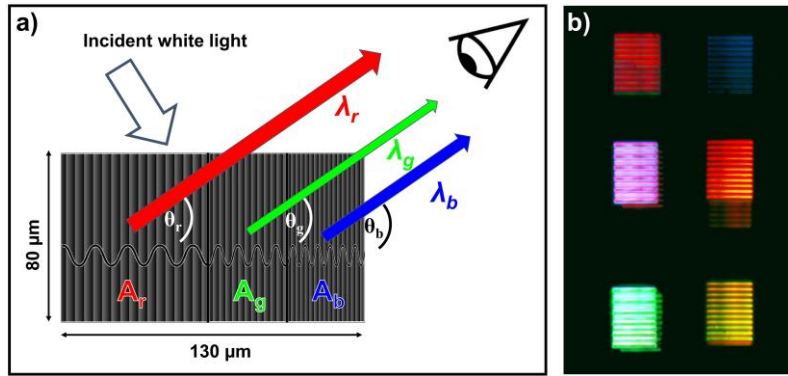


Figure 6. (a) Structured color by subdivision of SLM exposure frame into 3 regions with periods $d_r = 2.59 \mu\text{m}$, $d_g = 2.18 \mu\text{m}$, and $d_b = 2.0 \mu\text{m}$, respectively. Area of each region determines color weight in 1st order. (b) Six separate SRGs continuously printed and with six unique area compositions, viewed in first order with diffuse lighting.

The proportional intensity of each color is then determined by the areas A_r , A_g , and A_b . Figure 6(b) is an example showing 6 separate gratings designed to diffract a variety of colors simply by altering the relative areas A_r , A_g , and A_b .

The gratings are 10 stripes of $130\text{ }\mu\text{m} \times 80\text{ }\mu\text{m}$ printed along a 1.0 mm length; a space is inserted between each for visual clarity. For all, the SLM was divided into 3 regions with periods of $d_r = 2.59\text{ }\mu\text{m}$, $d_g = 2.18\text{ }\mu\text{m}$, and $d_b = 2.0\text{ }\mu\text{m}$, respectively.

4. DISCUSSION

We have exploited recent advances in digital polarization optics and photomechanically-responsive azopolymers to demonstrate the continuous laser-printing of surface microstructures, using the translational speed as a primary driver of the depth modulation. For the speeds used here, 25 mm^2 sinusoidal relief gratings of $2.0\text{ }\mu\text{m}$ period and amplitudes up to 670 nm were fabricated. The total fabrication time of these gratings ranged from 2 hours to 24 hours for the smallest and largest amplitude gratings, respectively. The relatively long 24 hour fabrication is considerably mitigated because of the minimal environmental restrictions on the writing process. The inherently sluggish photomechanical response of the azopolymer makes the fabrication immune to the acoustic, optical, and mechanical disturbances that severely impact related optical lithographic techniques that rely on photochemical processes. The gratings presented here were all fabricated in ambient room light on an open optical bench with only passive vibration isolation. A related and more powerful mitigating factor is likewise rooted in the slow photomechanical response- namely, because the surface grating process originates in the slow movement of polymer mass, the continuous translation of the film during the writing process provides a beneficial averaging effect, producing uniform amplitude profiles with variations less than $\pm 4\%$. Indeed, this variation itself may originate in minor motor speed and/or laser power variations and is the subject of ongoing investigation.

In summary, we have demonstrated a new process to laser-print surface relief gratings on azopolymer films that is scalable to large area. Using an SLM to project structured polarized light onto the moving film surface, sinusoidal SRGs of programmable period can be written and used immediately after fabrication for replication using nanoimprint lithography.

ACKNOWLEDGMENTS

The authors acknowledge support from the US National Science Foundation (NSF) Division of Electrical, Communications and Cyber Systems, award number 2024118, and NSF Division of Materials Research, award number 1919557.

REFERENCES

- [1] Kress, B.C. and Meyrueis, P., [Applied Digital Optics: From Micro-optics to Nanophotonics], John Wiley and Sons, Chichester, (2009).
- [2] Herzig, H. P. (Ed.), [Micro-Optics: Elements, Systems, and Applications], CRC Press, (1997).
- [3] Chan, Y. C., Lam, Y. L., Zhou, Y., Xu, F.L., Liaw, C., Jiang, W., and Ahn, J., "Development and applications of a laser writing lithography system for maskless patterning," Optical Engineering 37(9), 2521-2530 (1998).
- [4] Chen, C.G., Konkola, P.T., Heilmann, R.K., Pati, G.S., and Schattenburg, M.L., "Image metrology and system controls for scanning beam interference lithography," J. Vac. Sci. Technol. B 19, 2335–2341 (2001).
- [5] Rahlves, M., Kelb, C., Rezem, M., Schlangen, S., Boroz, K., Gödeke, D., Ihme, M., and Roth, B., "Digital mirror devices and liquid crystal displays in maskless lithography for fabrication of polymer-based holographic structures," Journal of Micro/Nanolithography, MEMS, and MOEMS 14(4), 041302 (2015).
- [6] You, S., Zhu, W., Wang, P., and Chen, S., "Projection printing of ultrathin structures with nanoscale thickness control," ACS Appl. Mater. Interfaces 11(17), 16059-16064 (2019).
- [7] Gale, M.T., Rossi, M., Pedersen, J. and Schuetz, H., "Fabrication of continuous-relief micro-optical elements by direct laser writing in photoresists," Optical Engineering 33(11), 3556-3566 (1994).
- [8] LeCompte, M., Gao, X., and Prather, D.W., "Photoresist characterization and linearization procedure for the gray-scale fabrication of diffractive optical elements," Appl. Opt. 40, 5921-5927 (2001).
- [9] Priimagi, A., and Shevchenko, A., "Azopolymer-based micro-and nanopatterning for photonic applications," J. Poly. Sci. B: Poly. Phys. 52(3), 163-182 (2014).

[10] Viswanathan, N.K., Kim, D.Y., Bian, S., Williams, J., Liu, W., Li, L., Samuelson, L., Kumar, J., Tripathy, S.K., "Surface relief structures on azo polymer films," *J. Mater. Chem.* 9(9), 1941–1955 (1999).

[11] Vapaavuori, J., Valtavirta, V., Alasaarela, T., Mamiya, J., Priimagi, A., Shishido, A., and Kaivola, M, "Efficient surface structuring and photoalignment of supramolecular polymer-azobenzene complexes through rational chromophore design," *J. Mat. Chem.* 21(39), 15437-15441 (2011).

[12] Barrett, C.J., Mamiya, J.I., Yager, K., and Ikeda, T., "Photo-mechanical effects in azobenzene-containing soft materials," *Soft Matter* 3(10), 1249-1261 (2007).

[13] Salvatore, M., Oscurato, S.L., Maddalena, P. and Ambrosio, A., "Light-induced complex surface structuring of azobenzene-containing materials," in *Advances in Nanostructured Materials and Nanopatterning Technologies*, 273-296, Elsevier (2020).

[14] Kim, D.Y., Tripathy, S.K., Li, L., and Kumar, J., "Laser-induced holographic surface relief gratings on nonlinear optical polymer films," *Appl. Phys. Lett.* 66(10), 1166–1168 (1995).

[15] Kulikovska, O., Goldenberg, L.M., and Stumpe, J., "Supramolecular azobenzene-based materials for optical generation of microstructures," *Chem. Mater.* 19(13), 3343-3348 (2007).

[16] Oscurato, S.L., Salvatore, M., Borbone, F., Maddalena, P., and Ambrosio, A., "Computer-generated holograms for complex surface reliefs on azopolymer films," *Scientific Reports* 9(1), 6775 (2019).

[17] Strobel, J., Van Soelen, M., Abourahma, H., and McGee, D.J., "Supramolecular azopolymers for dynamic surface microstructures using digital polarization optics," *Adv. Optical Mater.* 11(8), 2202245, (2023).

[18] Strobel, J., Stolz, D., Leven, M., Van Soelen, M., Kurlandski, L., Abourahma, H., and McGee, D.J., "Optical microstructure fabrication using structured polarized illumination," *Opt. Express* 30(5), 7308, (2022).

[19] Reda, F., Salvatore, M., Astarita, M., Borbone, F., and Oscurato, S.L., "Reprogrammable holograms from maskless surface photomorphing," *Adv. Optical Mater.* 11(21), 2300823 (2023).

[20] Krüger, J., Bolle, N., Calvelo, T., Bergmann, S., Abourahma, H., and McGee, D.J., "Optical reconfiguration of surface relief gratings on supramolecular polymer films using grating translation and superposition," *J. Appl. Phys.* 125, 243108 (2019).

[21] Rekola, H., Berdin, A., Fedele, C., Virkki, M., and Priimagi, A., "Digital holographic microscopy for real-time observation of surface-relief grating formation on azobenzene-containing films," *Scientific Reports* 10(1), 19642 (2020).